Available online at www.sciencedirect.com
SCIENCE DIRECT
European Journal of Pharmaceutical Sciences 25 (2005) 455–465
EUROPEAN JOURNAL OF PHARMACEUTICAL SCIENCES
www.elsevier.com/locate/ejps

Transport of nanoparticles across an in vitro model of the human intestinal follicle associated epithelium

Anne des Rieux [a,b,c,*], Eva G.E. Ragnarsson [a], Elisabet Gullberg [a], Véronique Préat [b], Yves-Jacques Schneider [c], Per Artursson [a]

[a] *Department of Pharmacy, Uppsala University, Uppsala, Sweden*
[b] *Unité de Pharmacie Galénique, Université catholique de Louvain, Avenue E. Mounier, 73-20, 1200 Brussels, Belgium*
[c] *Laboratoire de Biochimie Cellulaire, Institut des Sciences de la Vie, Université catholique de Louvain, Place L. Pasteur, 1, 1348 Louvain-La-Neuve, Belgium*

Received 29 October 2004; received in revised form 15 March 2005; accepted 14 April 2005

Abstract

An in vitro model of the human follicle associated epithelium (FAE) was characterized and the influence of nanoparticle properties on the transcellular transport across the in vitro model was investigated. The model was established by co-culturing Caco-2 and Raji cells, with Caco-2 cells alone as control. The conversion of Caco-2 cells to follicle associated epithelium (FAE) like cells was monitored by following the surface expression of β1-integrins (immunofluorescence) and nanoparticle transport (flow cytometry). The influence of the nanoparticle concentration at the apical side, temperature, size and surface properties of nanoparticles on transport was evaluated, as well as the influence of transport conditions. The conversion of Caco-2 cells into FAE-like cells occurred. The transport was concentration, temperature and size-dependent. Aminated nanoparticles were more efficiently transported than carboxylated nanoparticles, suggesting a role of nanoparticle surface functional groups and hydrophobicity, possibly leading to a different pattern of protein adsorption at their surface. In conclusion, this in vitro model is a promising tool to study the role of M cells in transintestinal nanoparticle transport, as well as to evaluate new drug delivery systems.

Keywords: M cells; Caco-2 cells; In vitro model; Oral delivery; Nanoparticles

1. Introduction

Drug delivery by the oral route is considered as the preferred route of administration, due to its convenience. It is user-friendly and reduces the risk of infection, as well as the pain for the patient, and possible contamination of the medical personnel. The intestinal epithelial barrier consists of a cell monolayer, predominantly composed of enterocytes interspersed by mucus-secreting goblet cells, that generally constitutes effective barriers, and prevents the uptake of microorganisms and other particles. Scattered throughout the gastrointestinal mucosa, the organized mucosa associated lymphoid tissues (O-MALT) is found (Clark et al., 2001b). O-MALT consists of lymphoid follicles arranged either singly or as clusters to form distinct structures, such as the Peyer's patches, situated immediately below the intestinal epithelial cell monolayer. These structures are separated from the lumen by the follicle associated epithelium (FAE), which differs from the normal intestinal epithelium in that it contains specialized epithelial M cells with the capacity to transport particulate matters, such as bacteria and viruses. These particular cells are mainly found in the FAE, although recently M cells have been identified in the villous epithelium and demonstrated to develop

Abbreviations: FAE, follicle associated epithelium; TEER, transepithelial electrical resistance; O-MALT, organized mucosa associated lymphoid tissues

* Corresponding author. Tel.: +32 2 764 73 21; fax: +32 2 764 73 98.
E-mail address: anne.desrieux@farg.ucl.ac.be (A.d. Rieux).

0928-0987/$ – see front matter © 2005 Elsevier B.V. All rights reserved.
doi:10.1016/j.ejps.2005.04.015

without the influence of the O-MALT structures (Jang et al., 2004).

The M cells are specialized for antigen sampling, but they are also exploited as a route of host invasion by many pathogens (Gebert et al., 1996; Kraehenbuhl and Neutra, 2000). Furthermore, M cells represent a potential portal for oral delivery of peptides and for mucosal vaccination, since they possess a high transcytotic capacity and are able to transport a broad range of materials, including nanoparticles (Clark et al., 2000; Frey and Neutra, 1997). However, despite the advantages of the oral route, most peptide and protein drugs as well as peptidomimetics available today are administered parenterally rather than orally. Their possible gastrointestinal degradation by digestive enzymes (Chen and Langer, 1998) and their very poor intestinal absorption (except for most peptides with no more than three or four amino acids) lead to a low oral bioavailability of such molecules. Because of the high potential and promising field that therapeutic peptides and proteins represent, new oral formulations have to be developed to tackle these difficulties. One delivery strategy could be based on the encapsulation of peptides in particulate carriers (liposomes, nano- or microparticles). This would protect the peptides against chemical and enzymatic degradation and potentially also enhance the selective uptake of these particles by M cells (Clark et al., 2001b).

Numerous studies have been performed on M cells to understand the strategies used by pathogens to exploit this pathway and to use their transport abilities for the delivery of vaccines to the mucosal immune system (Clark et al., 2001b; Frey and Neutra, 1997; Hussain and Florence, 1996; Kraehenbuhl and Neutra, 2000; Neutra et al., 1999; Owen, 1999). However, the more precise role played by M cells in the immune response, as well as the mechanisms of particle uptake and transport, remains poorly understood. In addition, only few specific markers of human M cells, e.g. the sialyl Lewis A antigen and cathepsin E (Finzi et al., 1993; Giannasca et al., 1999; Wong et al., 2003) have been identified. However, these results have not been confirmed since (Wong et al., 2003) and it remains difficult to identify and localize human M cells, limiting the progress in this field. Moreover, in vivo studies are difficult to perform and not always relevant due to the high variability of proportion and phenotype of M cells among different species (Brayden and Baird, 2001; Jepson et al., 1996).

An in vitro model was proposed (Kerneis et al., 1997) based on a “mixed” co-culture system of Caco-2 cells on inverted inserts and isolated lymphocytes from mouse Peyer’s patches. To overcome the use of primary murine lymphocytes, a new cell culture system has been developed to mimic the human FAE (Gullberg et al., 2000). It is based on the co-culture of Caco-2 cells on normally oriented inserts and human Raji B lymphocytes. Since our final objective is to study the oral delivery of vaccines or drugs designated to humans, the most relevant system for our application was the one developed by Gullberg et al. (2000).

Working with these in vitro models, the influence of the particle size (Gullberg et al., 2000), the temperature and the duration of exposure (Caliot et al., 2000; Ouzilou et al., 2002) on particle transcytosis through M cells was demonstrated. The influence of particle charge and hydrophobicity on transcytosis across M cells was also studied in vivo. In two independent studies, particles with a relatively high hydrophobicity were found to be absorbed more readily into mouse or rat Peyer’s patches (Eldridge et al., 1990; Hillery and Florence, 1996). In a third study (Keegan et al., 2003), a lower uptake of negatively charged polystyrene particles compared to non-ionized ones was observed in rats.

In this study, we investigated the influence of the physicochemical properties of the nanoparticles on particle transport across the human in vitro model of FAE, based on a co-culture of Caco-2 cells and human Raji B lymphocytes, developed by Gullberg et al. (2000). The influence of the nanoparticle concentration, the duration of incubation and the temperature on the particular transport across these cells, as well as the presence or absence of serum during transport experiments was also investigated.

2. Materials and methods

2.1. Materials

2.1.1. Cell lines

Human colon carcinoma Caco-2 line (clone 1), obtained from Dr. Maria Rescigno, University of Milano-Bicocca, Milano, Italy (Rescigno et al., 2001), from passage $x+6$ to $x+10$, and human Burkitt’s lymphoma Raji B line (American Type Culture Collection, Manassas, VA) from passage 102 to 104, unless stated, were used.

2.1.2. Cell culture media and chemicals

Dulbecco modified Eagle’s minimal essential medium (DMEM, 25 mM glucose), RPMI 1640 medium, heat inactivated fetal calf serum, non-essential amino acids, L-glutamine and penicillin-streptomycin (PEST) were purchased from Gibco™ Invitrogen Corporation (Carlsbad, CA). Trypsin-EDTA consisted in 2.5% (w/v) of trypsin (Gibco™) and 0.2% (w/v) EDTA (IGN, Aurora, OH) in PBS (Gibco™). Hank’s Balanced Salt Solution buffer (HBSS) 10× was obtained from Gibco™, Hepes, and sodium bicarbonate from Sigma (St. Louis, MO). Rhodamine-phalloidine was obtained from Molecular Probes (Eugene, OR). Citric acid, urea, CHAPS and Triton, were purchased from Sigma. The Iso Electric Focusing gel Pharmalyte 3-10, and dithiothreitol (DTT) were from Amersham Biosciences (Uppsala, Sweden). Pefabloc® SC was from Roche (Indianapolis, IN).

2.1.3. Cell culture reagents, nanoparticles and antibodies

Transwell® polycarbonate inserts (12 wells, pore diameter of 3 μm, polycarbonate) were purchased from Corning

Costar (New York, NY). Inserts were coated with Matrigel™ Basement Membrane Matrix (Becton Dickinson, Bedford, MA). Yellow-green carboxylated or aminated latex particles (FluoSpheres®) with mean diameters of 0.2 and 0.5 μm were obtained from Molecular Probes. The Monoclonal antibody to CD29 (integrin β1 subunit) was from BioGenex (San Ramon, CA). The Alexa Fluor 488 goat anti-mouse IgG1 was purchased from Molecular Probes. Rose Bengal was obtained from Aldrich.

2.2. Methods

2.2.1. Cell culture

Caco-2 cells were grown in flasks in DMEM supplemented with 10% (v/v) fetal calf serum, 1% (v/v) non-essential amino-acids and 1% (v/v) L-glutamine, at 37 °C under a 10% CO_2 water saturated atmosphere. Caco-2 cells were grown on inserts in the same medium further supplemented with 1% (v/v) PEST. Raji cells were cultivated in RPMI supplemented with 10% (v/v) fetal calf serum, 1% (v/v) non-essential amino-acids, 1% (v/v) L-glutamine and 1% (v/v) PEST, at 37 °C under a 5% CO_2 water saturated atmosphere.

Cells were co-cultivated following a previously described protocol (Gullberg et al., 2000). Briefly, Transwell® inserts were coated with Matrigel™, prepared in pure DMEM to a final protein concentration of 3.33 μg/ml. Three hundred microliters of this solution were poured on inserts (12 μg/cm^2) and placed at room temperature for 1 h. Supernatants were then removed and inserts washed with 500 μl of DMEM. 500 000 Caco-2 cells, suspended in 500 μl of supplemented DMEM + 1% (v/v) PEST, were seeded on the upper side of inserts and cultivated for 14 days. Then, 500 000 Raji cells, resuspended in supplemented DMEM + 1% (v/v) PEST, were added at the basolateral compartment of inserts. The co-cultures were maintained for 4–5 days. The medium of the upper compartment was changed every other day. Monocultures of Caco-2 cells, cultivated as above except for the presence of Raji cells, were used as controls.

2.2.2. Cell monolayer integrity

The cell monolayer integrity, both in co- and monocultures, was controlled by the transepithelial electrical resistance (TEER) measurement, performed with an Endohm™ tissue resistance chamber (Endohm-12, World Precision Instruments, Sarasota, FL) connected to a Millicell®-RES (Millipore, Billerica, MA) ohmmeter. The resistance of cell medium (18 Ω cm^2) was considered as a background and subtracted from each TEER value. The TEER values were usually approximately between 300 and 200 Ω cm^2 for mono- and co-cultures, respectively.

2.2.3. Particle transport

Transport experiments were run in HBSS buffered with 25 mM Hepes and 4 mM sodium bicarbonate, adjusted to pH 7.4 and supplemented with 1% (v/v) FCS unless otherwise stated. The concentration of nanoparticles was adjusted from the stock solution (checked by FACS analysis) by dilution in buffered HBSS supplemented or not with 1% (v/v) FCS, to a final concentration of 4.5×10^9 nanoparticles/ml unless otherwise stated and vortexed for 1 min to dissociate possible aggregates. The nanoparticle suspension was added to the apical side of cell monolayers (400 μl) and the inserts were incubated at 4 or 37 °C during the required duration of the experiment. Then, basolateral solutions were sampled and the number of transported particles was measured using a flow cytometer (FACScan, Becton Dickinson) (Gullberg et al., 2000). The measurements were based on both fluorescence and particle size. To assess the particle size and distribution, the used particles were analyzed on a NanoSZ (Malvern). The particle size was as expected and the populations were monodispersed (carboxylated nanoparticles: size = 210 nm, PDI = 0.006; aminated nanoparticles: size = 276, PDI = 0.032).

2.2.4. Localization of nanoparticles in the cell monolayer

After transport experiments, inserts were fixed on ice in 4% (v/v) buffered formaldehyde (pH 7.4, 10 min) and washed twice in 500 μl cold buffered HBSS. Actin was stained with 250 μl of rhodamine-phalloidine (1:75) in buffered HBSS + 0.2% (v/v) Triton X-100 for 10 min to reveal cell borders. Inserts were washed in buffered HBSS, cut and mounted on glass slides. Nanoparticle position in the cell monolayer was observed with a Leica™ TC4D confocal microscope. Data were analyzed by Image space™ software to obtain *y–z* and *x–y* views of the cell monolayers.

2.2.5. Immunofluorescence of β1-integrin

The cell monolayers were washed several times with buffered HBSS and fixed in 4% (v/v) buffered formaldehyde (10 min). After three washings in buffered HBSS, inserts were microwave-treated (2 × 10 min, 900 W) in 10 mM citrate buffer pH 6.0 and permeabilized with 0.2% (v/v) Triton X-100 in buffered HBSS for 5 min. Following further washing, cell monolayers were blocked under shaking in buffered HBSS supplemented with 2% (v/v) FCS (2 × 10 min, 100 rpm). They were then incubated for 2 h at 37 °C with an anti-CD29 (β1-integrin subunit) monoclonal antibody (dilution 1:50) in 0.02% (v/v) Triton X-100 in buffered HBSS. Then, inserts were washed repeatedly in buffered HBSS, incubated for 1 h with an Alexa Fluor® 488 goat anti-mouse IgG_1 (dilution 1:2000), washed again and mounted on glass slides. The slides were examined with a Leica™ TC4D confocal microscope.

2.2.6. Zeta potential

Zeta potential measurements were performed at 25 °C on a Malvern Zetasizer 2000 (Malvern, Worcestershire, UK). Polystyrene nanospheres (−50 ± 5 mV) (Duke Scientific Corp, Palo Alto, CA) were used to verify the perfor-

mance of the instrument. The zeta potential measurements of the nanoparticles were done in MilliQ water, buffered HBSS and buffered HBSS + 1% (v/v) FCS. Each nanoparticle dispersion was measured five times.

2.2.7. Surface hydrophobicity of nanoparticles

The surface hydrophobicity of amined- and carboxylated-decorated nanoparticles was measured by the Rose Bengal method, as previously described (Muller et al., 1997). Briefly, a known concentration of nanoparticles was diluted in a 20 μg/ml Rose Bengal solution and the adsorption of the hydrophobic Rose Bengal dye at the nanoparticle surface was evaluated by calculating the partitioning coefficient (PQ). The aqueous phase and the surface of the nanoparticles were considered as two phases.

The calculated PQ-value was plotted versus surface area. The surface hydrophobicity of the particles was evaluated by the slope of the line; the slope increases with increasing surface hydrophobicity.

2.2.8. 2D electrophoresis

2D polyacrylamide gel electrophoresis (2D PAGE) was used to determine and compare serum protein adsorption patterns on the carboxylate and amine-exposing particles. 1.8×10^{11} nanoparticles were incubated in 1 ml of pure FCS. After separation and washing of the particles (by centrifugation; three times in PBS), the pellet obtained was dispersed in a protein solubilizing solution containing 54% (w/v) urea, 4% (w/v) CHAPS, 0.1% (w/v) Pefabloc, 2% (v/v) Pharmalyte 3-10 and 1% (w/v) dithiothreitol (DTT) (Blunk et al., 1993) and placed at 90 °C during 5 min. Samples were then centrifuged and the supernatant containing the solubilized proteins was collected and analyzed. 2D PAGE was performed essentially as described previously (Hochstrasser et al., 1988). Fifty microliters of the solubilized protein solution were separated on the first-dimensional gel using carrier ampholytes (pH 3–10, voltage). After SDS-PAGE (12% polyacrylamide gel), the gels were silver-stained and scanned.

2.2.9. Statistics

The transport of particles across the co- and mono-cultured cell monolayers was compared using non-parametric tests: Mann–Whitney and Kruskall–Wallis tests (significance $P < 0.05$).

3. Results

3.1. Conversion of Caco-2 cells to FAE-like cells

3.1.1. Transport of yellow-green-conjugated carboxylated nanoparticles

In order to monitor the conversion of Caco-2 cells into FAE-like cells in the presence of Raji cells, the transport rate of 0.2 μm yellow-green-conjugated nanoparticles across mono- and co-cultures was studied (Gullberg et al., 2000). The nanoparticles were added apically and incubated with the cells at 37 °C for 90 min. The number of transported nanoparticles was significantly higher in co-cultures than in mono-cultures (7760 ± 4654 nanoparticles, versus 7 ± 11, respectively; $n = 3$, $P < 0.05$).

3.1.2. β1-Integrin expression

To identify the conversion of Caco-2 cells into FAE-like cells, immunofluorescence staining of β1-integrins was performed on cell monolayers. As reported previously, in Fig. 1, β1-integrins were located at the apical pole of FAE-like cells (co-cultures), whereas only a basolateral expression was observed in Caco-2 cells (mono-cultures) (Gullberg, 2005). Hence, the conversion of a part of the Caco-2 cells into FAE-like cells occurred and the co-culture system was functional.

3.2. Concentration-dependent transport

In order to evaluate whether the transport of nanoparticles by the FAE-like cells was concentration-dependent, three concentrations of nanoparticles (ranging from 10^5 to 10^9 nanoparticles/ml) were added at the apical side of the cell monolayers and incubated with the cells at 37 °C during 20 min. Fig. 2 illustrates that the number of nanoparticles transported by the co-cultures increased with the concentration of the donor solution (40× between 10^7 and 10^9 nanoparticles/ml) ($P < 0.05$).

3.3. Influence of incubation temperature

To investigate whether the transport of 0.2 μm yellow-green nanoparticles added at the apical pole of the cell monolayers was temperature-dependent, experiments were carried out at 4 and 37 °C. Besides a counting of the transported nanoparticles by FACScan, confocal observations were performed to visualize particles within the cell monolayers.

At 37 °C, the FAE-like cells transported a significantly higher number of fluorescent nanoparticles than the controls, whereas at 4 °C, the transport was reduced to the control range ($n = 3$, $P < 0.05$; Fig. 3).

Confocal microscopy showed (Fig. 4) that a lower number of nanoparticles were internalized in the FAE-like cells incubated at 4 °C for 60 min than at 37 °C for 90 min. At 4 °C, *y–z* orthogonal projections, allowing localization of nanoparticles within the cell monolayers, did not indicate any difference between mono- and co-cultures with very few nanoparticles detected at the cell monolayer surface or intracellularly. At 37 °C, the nanoparticles were mainly localized at the cell apical surface in mono-cultures, whereas in the co-cultures, more nanoparticles were internalized (Fig. 4).

3.4. Influence of particle size

To evaluate the effect of particle size on transport, yellow-green carboxylated nanoparticles of 0.2 and 0.5 μm

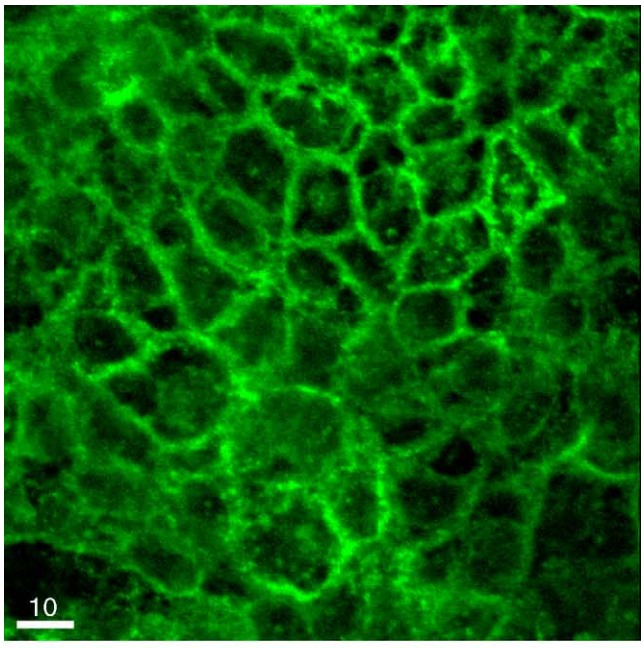

(A)

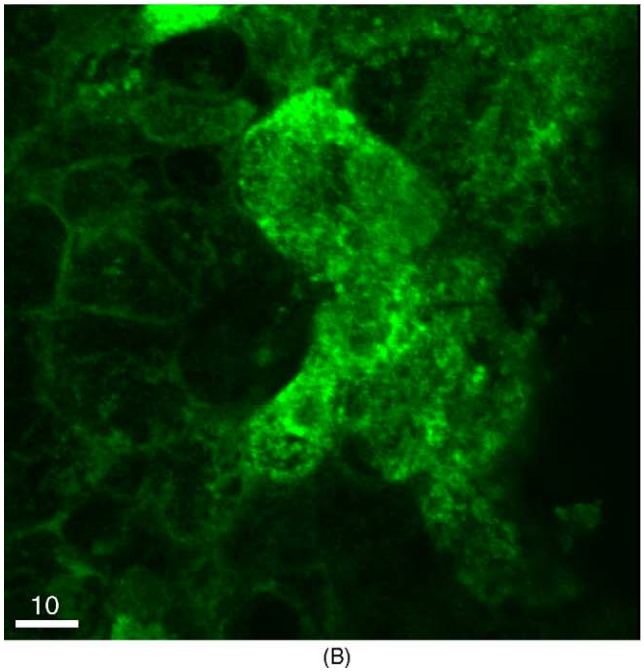

(B)

Fig. 1. Identification and localization of FAE-like cells by immunofluorescence staining of β1-integrins in mono-culture (A) and co-cultures (B), at the apical level, using confocal microscopy.

were added at the apical side of the cell monolayers. The cell monolayers were incubated with the nanoparticles at 37 °C for 120 min and the basolateral media sampled every 30 min to monitor the transport. Fig. 4 illustrates that after 120 min of incubation, whatever the size, the amount of nanoparticles transported in the mono-cultures remained lower than in the co-cultures. In the co-cultures, the number of nanoparticles that were transcytosed increased al-

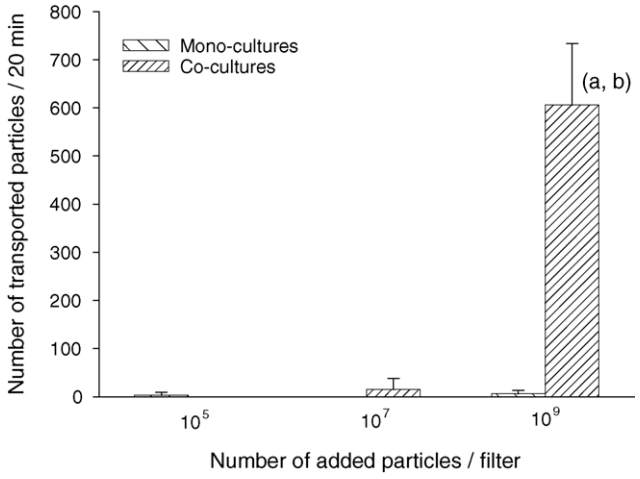

Fig. 2. Influence of the number of nanoparticles in the donor solution on the transport rate. Different concentrations (10^5, 10^7, 10^9 nanoparticles/filter) of yellow-green carboxylated nanoparticles (0.2 μm), suspended in buffered HBSS + 1% FCS, were added to the apical pole of the cell monolayers. Mono- and co-cultures were incubated with yellow-green carboxylated nanoparticles for 20 min at 37 °C and the number of transported nanoparticles was evaluated by flow cytometry ($n = 4$). (a) The transport of particles was significantly higher in the co-cultures compared with the mono-cultures when incubated with the 10^9 nanoparticles/ml solution, $P < 0.05$. (b) The transport of particles was significantly higher in the co-cultures incubated with the 10^9 nanoparticles/ml solution compared with the co-cultures incubated with the 10^7 nanoparticles/ml solution, $P < 0.05$.

most proportionally with the duration of incubation. The number of 0.2 μm transported nanoparticles was seven times higher ($P < 0.05$) than that of 0.5 μm nanoparticles (Fig. 5).

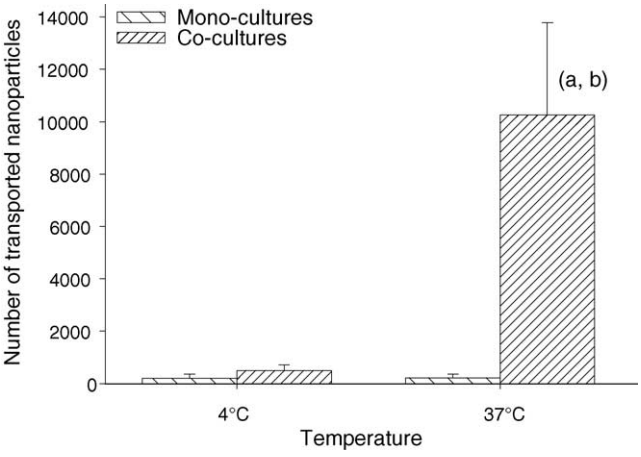

Fig. 3. Influence of temperature on nanoparticle transport: quantification of the number of transported nanoparticles. Mono- and co-cultures were incubated with yellow-green carboxylated nanoparticles for 60 min at 4 °C and then at 37 °C during 90 min. The number of transported nanoparticles was evaluated by flow cytometry ($n = 3$). (a) The transport of particles was significantly higher in the co-cultures compared with the mono-cultures when incubated at 37 °C, $P < 0.05$. (b) The transport of particles was significantly higher in the co-cultures incubated at 37 °C compared with the co-cultures incubated at 4 °C, $P < 0.05$.

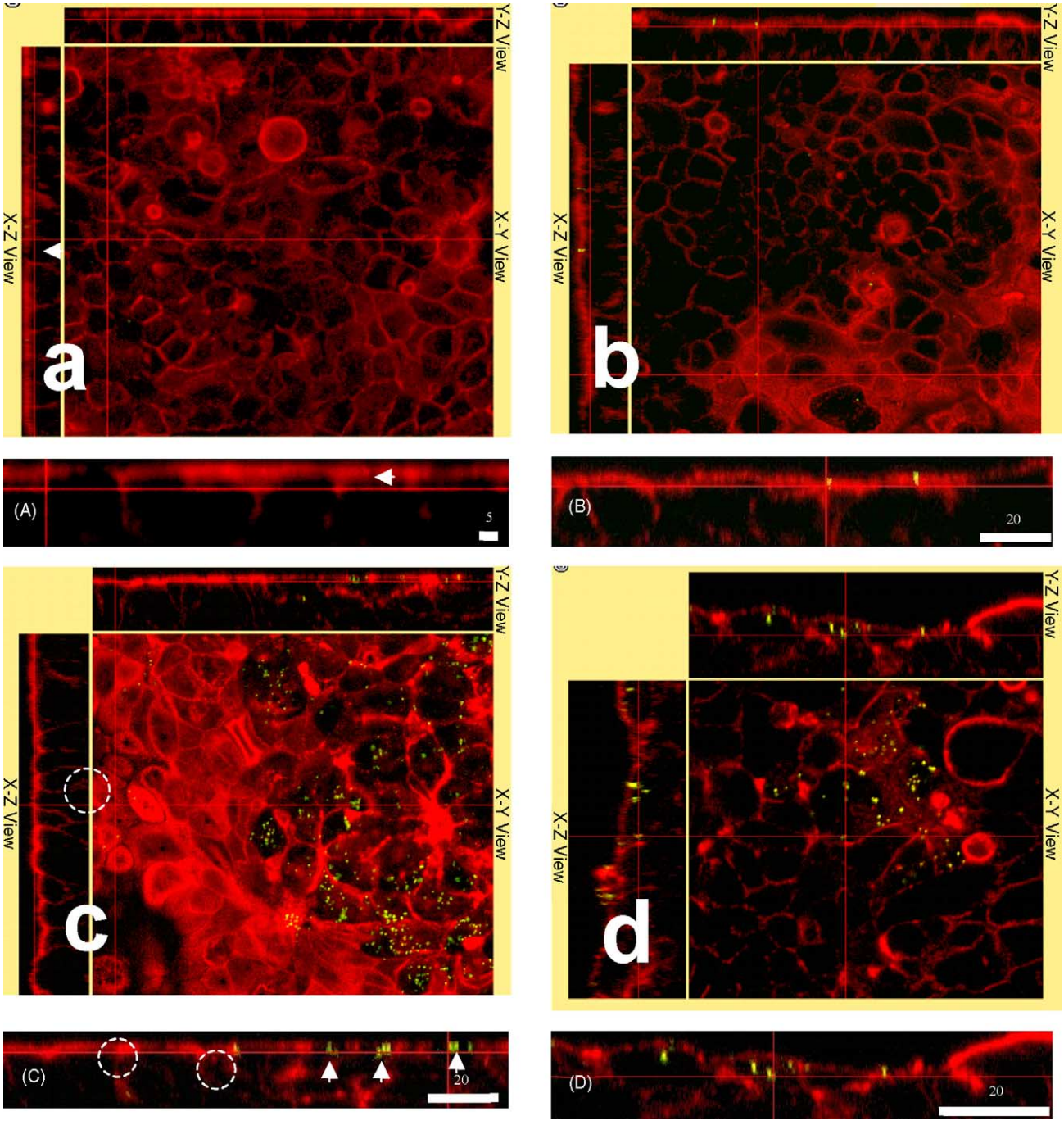

Fig. 4. Influence of temperature on nanoparticle transport: localization of nanoparticles in cell monolayers. Cells were stained with rhodamine-phalloidine (red) and beads were yellow-green-labelled. Mono- and co-cultures were fixed and stained after incubation with yellow-green carboxylated 0.2 μm beads at 4 °C during 60 min (pictures a and b), and then at 37 °C during 90 min (pictures c and d). Mono-cultures were used as controls. Red lines indicate where, within the cell monolayers, the pictures were taken and analyzed. The arrows and circles indicate the nanoparticle localization in the cell monolayers. (For interpretation of the references to color in this figure legend, the reader is referred to the web version of the article.)

3.5. Influence of the surface functional groups of nanoparticles

To evaluate the effect of the surface functional groups on particles transport, 0.2 μm yellow-green nanoparticles exposing either carboxylic or amino groups were compared. After 90 min of incubation, the amount of particles transported in the co-cultures was higher than in the mono-cultures, independently of the surface properties of the nanoparticles ($P < 0.05$, Fig. 6). The results were here expressed in percentages of the donor solution, since the concentration of the donor solution of carboxylated nanoparticles was different from the one of aminated nanoparticles. In the co-cultures, the transport of both types of nanoparticles increased propor-

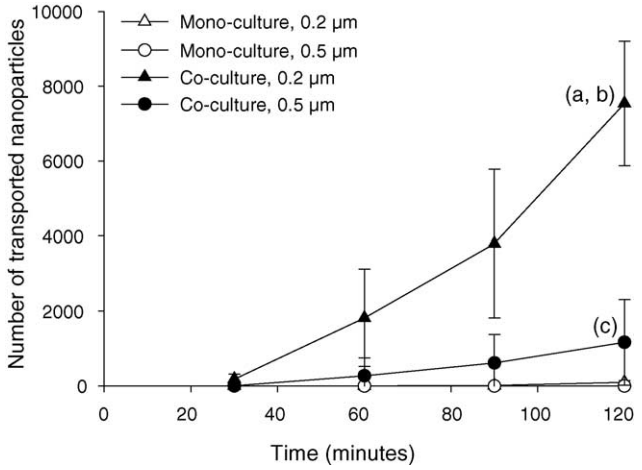

Fig. 5. Influence of particle size on nanoparticle transport. Yellow-green carboxylated nanoparticles of different size (0.2 and 0.5 μm), suspended in buffered HBSS + 1% FCS, were added to the apical pole of the cell monolayers and incubated for 90 min at 37 °C. The transport kinetics were compared ($n = 4$). (a) The transport of particles was significantly higher in the co-cultures compared with the mono-cultures when incubated with the 0.2 μm nanoparticles, $P < 0.05$. (b) The transport of particles was significantly higher in the co-cultures incubated with the 0.2 μm nanoparticles compared with the co-cultures incubated with the 0.5 μm nanoparticles, $P < 0.05$. (c) The transport of particles was significantly higher in the co-cultures compared with the mono-cultures when incubated with the 0.5 μm nanoparticles, $P < 0.05$.

tionally with the duration of incubation and the nanoparticles having cationic sites were transported to a larger extent than those with anionic sites ($P < 0.05$, Fig. 6A). We conclude that the chemical properties of the particle surface played a direct or indirect role in the binding, uptake and transcytosis across the FAE model.

3.6. Influence of the surface properties of nanoparticles

In order to investigate the influence of the surface properties of nanoparticles on their transport by M cells, the zeta potential of the nanoparticle was measured. The measurements were done in deionizer water, buffered HBSS and buffered HBSS + 1% FCS (transport conditions) (Table 1). In water, carboxylated nanoparticles were highly negatively charged. Surprisingly, amined particles were also negatively charged, though to a lower extent than the carboxylated particles. X-ray photoelectron spectroscopy (XPS) analysis (data not shown) further confirmed the presence of free carboxylic functions as well as amine functions at the aminated nanoparticle surface. In buffered HBSS the difference between the two types of nanoparticles decreased. Finally, in the presence of serum, both the carboxylated and the aminated nanoparticles had the same zeta potentials and were slightly negatively charged. Hence, the difference observed in the transport in the presence of FCS between the two kinds of nanoparticles could not directly be explained by the different electrical properties of the nanoparticles.

Then, the surface hydrophobicity of aminated and carboxylated nanoparticles was analyzed, using a colorimetric test based on the Rose Bengal assay (Muller et al., 1997). Aminated nanoparticles appeared more hydrophobic compared to carboxylated ones (Fig. 7). This observation was consistent with less negative zeta potential values of the aminated nanoparticles.

3.7. Influence of transport conditions

In order to further investigate factors influencing the nanoparticle transport, different medium conditions were studied. Transport experiments with 0.2 μm yellow-green carboxylated and aminated nanoparticles were carried out in either serum containing or serum-free transport medium (buffered HBSS) (Fig. 6). After 90 min at 37 °C, the number of transported nanoparticles, either aminated carboxylated ones, across the co-cultures was significantly higher in the absence than in presence of serum ($P < 0.05$, Fig. 6B and C). These observations enlightened the influence of serum proteins on transport. Consequently, on the basis of these results, it was hypothesized that differential absorption of serum proteins at the two different particle surfaces could influence the transport rate across M cells. On this assumption, proteins that adsorbed at the surface of carboxylated and aminated nanoparticles were analyzed by 2D electrophoresis. Serum proteins were incubated with the two types of nanoparticles. After washing, the adsorbed proteins were analyzed upon 2D electrophoresis and slightly different patterns were observed (Fig. 8), suggesting that the type of adsorbed protein could influence the rate of transcytosis of the particle across M cells.

These data underlined the importance of particle surface properties on their transport by M cells.

4. Discussion

To characterize the in vitro model of the human FAE, the influence of several parameters like particle concentration at the apical side of the cells, particle size, temperature, duration of incubation and presence of serum on the nanoparticle transport was studied. We confirmed the observations already done in vitro (Caliot et al., 2000; Ouzilou et al., 2002)

Table 1
Zeta potential of carboxylated and aminated nanoparticles measured in three different conditions

ζ (mV)	Deionized water	Buffered HBSS	Buffered HBSS + 1% FCS
Carboxylated particles	−39 ± 0.3[a]	−35.4 ± 2.6[a]	−13.7 ± 0.9[a]
Aminated particles	−12.3 ± 0.4[a]	−28.7 ± 0.4[a]	−14 ± 2.4[a]

[a] S.D., $n = 5$.

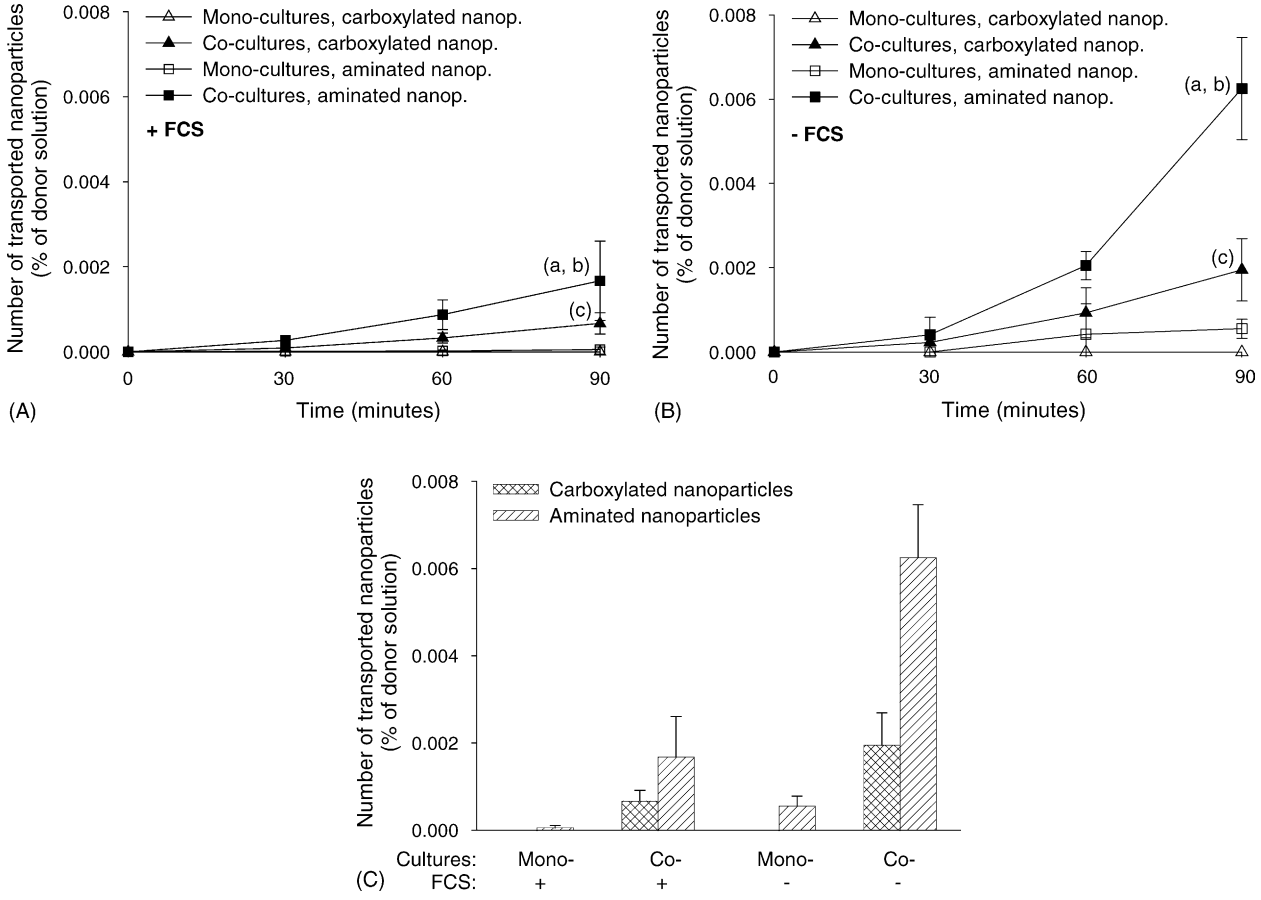

Fig. 6. (A) Influence of surface properties of particles, in the presence of fetal calf serum. Yellow-green carboxylated and aminated nanoparticles, suspended in buffered HBSS + 1% FCS, were added to the apical pole of the cell monolayers and incubated for 90 min at 37 °C. The transport kinetics were compared ($n = 5$). Results are expressed in percentages of the donor solutions. (a) The transport of particles was significantly higher in the co-cultures compared with the mono-cultures when incubated with the aminated nanoparticles, $P < 0.05$. (b) The transport of particles was significantly higher in the co-cultures incubated with the aminated nanoparticles compared with the co-cultures incubated with carboxylated nanoparticles, $P < 0.05$. (c) The transport of particles was significantly higher in the co-cultures compared with the mono-cultures when incubated with the carboxylated nanoparticles, $P < 0.05$. (B) Influence of surface properties of particles, in the absence of fetal calf serum. Yellow-green carboxylated and aminated nanoparticles, suspended in buffered HBSS without FCS, were added apically to cell monolayers and incubated 90 min at 37 °C. The transport kinetics were compared ($n = 3$). Results are expressed in percentages of the donor solutions. (a) The transport of particles was significantly higher in the co-cultures compared with the mono-cultures when incubated with the aminated nanoparticles, $P < 0.05$. (b) The transport of particles was significantly higher in the co-cultures incubated with the aminated nanoparticles compared with the co-cultures incubated with carboxylated nanoparticles, $P < 0.05$. (c) The transport of particles was significantly higher in the co-cultures compared with the mono-cultures when incubated with the carboxylated nanoparticles, $P < 0.05$. (C) Influence of serum on transport of particle by co-cultures. Transport of 0.2 μm yellow-green carboxylated and aminated nanoparticles in the presence or absence of serum; incubation for 90 min at 37 °C ($n = 3$). Results are expressed in percentages of the donor solutions.

and in vivo (Beier and Gebert, 1998; Keegan et al., 2003) that the transport is temperature-dependent, suggesting an energy-dependent transport, as well as proportional to the duration of contact. In addition we found that the transport was concentration-dependent too, as shown by the increased transport when higher quantities of particles are added to the apical side.

Different systems have been used to investigate drug delivery to M cells. These include liposomes (Clark et al., 2001a) and nanospheres of biodegradable and biocompatible polymers (Thanou et al., 2001; Vila et al., 2002). The surface properties of the particles were identified as crucial for the success of the delivery, although the optimal properties for M cell targeting remains undefined (Florence et al., 1995; Vila et al., 2002). It has already been demonstrated that, in rats, carboxylated microspheres were taken up to a lesser degree than the non-ionized particles (Jani et al., 1989) and that positively charged particles were more absorbed than the neutral or negatively ones (Janes et al., 2001). Here we show that the presence of cationic groups at the particle surface enhances their transport through FAE-like cells. This could be explained by the electrostatic interaction between the cationic particle surface and anionic structures, e.g. proteoglycans, on the cell surface (Ruponen et al., 2004). Surprisingly, the zeta potentials of these particles, in the presence of serum, were negative and equivalent to the zeta potential of the carboxylated particles. The surface hydrophobicity of nanoparticles was then investigated, enlightening a difference between the

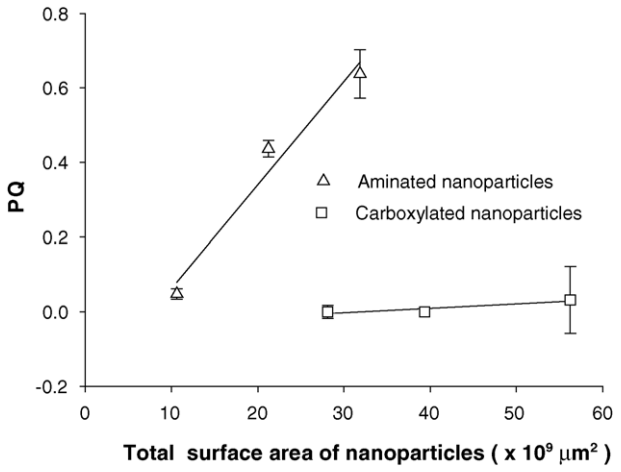

Fig. 7. Analysis of the nanoparticle surface hydrophobicity by the Rose Bengal method. Carboxylated and aminated nanoparticles were incubated with a 20 μg/ml Rose Bengal solution and centrifuged. The partitioning coefficient (PQ) was calculated. The aqueous phase and the surface of the nanoparticles were considered as two phases. The PQ of aminated nanoparticles was significantly higher compared with the PQ of carboxylated nanoparticles, $P < 0.05$.

two types of nanoparticles used. Surface hydrophobicity is known as an important factor influencing the nanoparticle transport by M cells (Eldridge et al., 1990; Jepson et al., 1993a, 1993b). It was then hypothesized that the hydrophobicity of nanoparticle surface might have an indirect impact on the transcytosis rate by conditioning the pattern of adsorbed proteins at the surface of the nanoparticles (Gessner et al., 2002). This could possibly lead to different binding and uptake mechanisms, which in turn influence the efficiency of nanoparticle transport. This hypothesis was supported by a higher transport of nanoparticles in absence of serum. Preliminary investigations using 2D gel electrophoresis showed that the proteins adsorbed at the nanoparticle surface differed, but the exact composition of the adsorbed proteins remains to be elucidated. It has been shown that extracellular fluids, e.g. mucus covering the intestinal epithelium, contains a mixture of proteins (40%) (Larhed et al., 1998), composed of a considerable amount of albumin as well as IgA (Kraehenbuhl and Neutra, 1992; Lentner, 1981) Those extracellular proteins can possibly adsorb to surfaces of cationic drug delivery systems and thereby decrease their adsorption and uptake, making more necessary a specific targeting of the drug formulation to the cells of interest. It would be then very important when elaborating drug delivery systems to find an adequate balance between all these factors to promote as much as possible their transport by the M cell.

Concerning the absolute values of the number of transported beads, variations have been observed between the experiments (7500–12 000/insert for co-cultures and 0–200/insert for mono-cultures). This is probably a result of the variable number of Caco-2 cells converted into FAE-like cells between experiments, emphasizing the need of a method evaluating the Caco-2 cell conversion rate in FAE-like cells. However, the order of magnitude of the number of transported nanoparticles – in similar conditions – is constant comparing the different experiments (around 10 000 for the co-cultures and around 100 for the mono-cultures at 37 °C

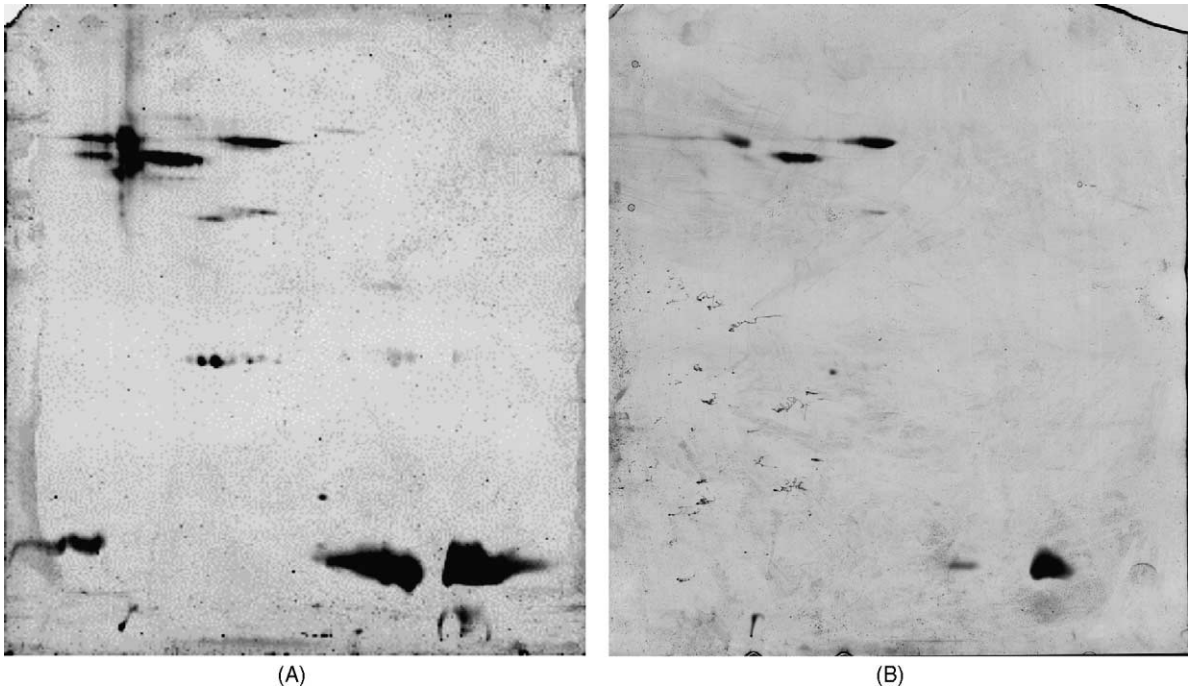

Fig. 8. 2D electrophoresis gels of serum proteins adsorbed at the carboxylated and aminated nanoparticle surface. Carboxylated (A) and aminated (B) nanoparticles were incubated for 1 h in 100% FCS and washed three times in PBS. Then the adsorbed proteins were removed from the nanoparticle surface and analyzed in 2D electrophoresis. Proteins were silver-stained.

during 90 min, in the presence of serum) and, secondly, the results obtained in two different laboratories (Department of Pharmacy, Uppsala & Laboratoire de Biochimie cellulaire, Louvain-la-Neuve) are comparable.

At last, this model allows discrimination between nanoparticles with different characteristics and allows the identification of important criteria influencing the transcytosis. Consequently, this model will be very useful to assess new formulations to oral administration of therapeutic peptides or vaccines.

Acknowledgments

The authors thank Dr. Göran Ocklind, from the Division of Pharmaceutics of the Uppsala University, and Prof. Claude Remacle from the Université catholique de Louvain for their scientific and technical support in the realization of confocal analysis as well as Dr. Lucia Lazorova, from the Division of Pharmaceutics of the Uppsala University, for her precious help and knowledge sharing in cell culture matters. The authors wish to thank Dr. Sandrine Horman from the Christian de Duve Institute of Cellular Pathology for her scientific and technical support in the realization of 2D electrophoresis gels, as well as André Tonon from the Ludwig Institute Cancer Research for his support in the realization of FACScan analysis. We thank Prof. Jo Demeester from the Gent University for allowing the realization of zeta potential measurements in his laboratory. Bernard Ucakar is acknowledged for their technical support as well as Jean-Pierre Vandiest for his help with the figures. The authors will at last thank Dr. J. Van Gelder, Dr. A. Cauvin and M. Oth from Lilly© for interest and support of the project. This work was supported by the Region Wallonne (DGTRE), First Europe (no. 215099), by the Fond Scientifique de Recherche of the Université catholique de Louvain and by a grant from National Network for Drug Development of the Swedish Foundation for Strategic Research to E.R.

References

Beier, R., Gebert, A., 1998. Kinetics of particle uptake in the domes of Peyer's patches. Am. J. Physiol. Gastrointest. Liver Physiol. 275, G130.

Blunk, T., Hochstrasser, D.F., Sanchez, J.C., Muller, B.W., Muller, R.H., 1993. Colloidal carriers for intravenous drug targeting: plasma protein adsorption patterns on surface-modified latex particles evaluated by two-dimensional polyacrylamide gel electrophoresis. Electrophoresis 14, 1382–1387.

Brayden, D.J., Baird, A.W., 2001. Microparticle vaccine approaches to stimulate mucosal immunisation. Microbes Infect. 3, 867–876.

Caliot, E., Libon, C., Kerneis, S., Pringault, E., 2000. Translocation of ribosomal immunostimulant through an in vitro-reconstituted digestive barrier containing M-like cells. Scand. J. Immunol. 52, 588–594.

Chen, H., Langer, R., 1998. Oral particulate delivery: status and future trends. Adv. Drug Deliv. Rev. 34, 339–350.

Clark, M.A., Blair, H., Liang, L., Brey, R.N., Brayden, D., Hirst, B.H., 2001a. Targeting polymerised liposome vaccine carriers to intestinal M cells. Vaccine 20, 208–217.

Clark, M.A., Hirst, B.H., Jepson, M.A., 2000. Lectin-mediated mucosal delivery of drugs and microparticles. Adv. Drug Deliv. Rev. 43, 207–223.

Clark, M.A., Jepson, M.A., Hirst, B.H., 2001b. Exploiting M cells for drug and vaccine delivery. Adv. Drug Deliv. Rev. 50, 81–106.

Eldridge, J.H., Hammond, C.J., Meulbroek, J.A., Staas, J.K., Gilley, R.M., Tice, T.R., 1990. Controlled vaccine release in the gut-associated lymphoid tissues. I. Orally administered biodegradable microspheres target the Peyer's patches. J. Contr. Release 11, 205–214.

Finzi, G., Cornaggia, M., Capella, C., Fiocca, R., Bosi, F., Solcia, E., Samloff, I.M., 1993. Cathepsin E in follicle associated epithelium of intestine and tonsils: localization to M cells and possible role in antigen processing. Histochemistry 99, 201–211.

Florence, A.T., Hillery, A.M., Hussain, N., Jani, P.U., 1995. Nanoparticles as carriers for oral peptide absorption: studies on particle uptake and fate. J. Contr. Release 36, 39–46.

Frey, A., Neutra, M.R., 1997. Targeting of Mucosal Vaccines to Peyer's Patch M Cells. Behring Institute Mitteilungen, pp. 376–389.

Gebert, A., Rothkotter, H.J., Pabst, R., 1996. M cells in Peyer's patches of the intestine. Int. Rev. Cytol. 167, 91–159.

Gessner, A., Lieske, A., Paulke, B., Muller, R., 2002. Influence of surface charge density on protein adsorption on polymeric nanoparticles: analysis by two-dimensional electrophoresis. Eur. J. Pharm. Biopharm. 54, 165–170.

Giannasca, P.J., Giannasca, K.T., Leichtner, A.M., Neutra, M.R., 1999. Human intestinal M cells display the sialyl Lewis A antigen. Infect. Immun. 67, 946–953.

Gullberg, E., Leonard, M., Karlsson, J., Hopkins, A.M., Brayden, D., Baird, A.W., Artursson, P., 2000. Expression of specific markers and particle transport in a new human intestinal M-cell model. Biochem. Biophys. Res. Commun. 279, 808–813.

Gullberg, E., 2005. Particle Transcytosis across the Human Intestinal Epithelium—Model Development and Target Identification for Improved Drug Delivery. Comprehensive Summaries of Uppsala Dissertations from the Faculty of Pharmacy, 3. Acta Universitatis Upsaliensis, Uppsala, Sweden.

Hillery, A.M., Florence, A.T., 1996. The effect of adsorbed poloxamer 188 and 407 surfactants on the intestinal uptake of 60-nm polystyrene particles after oral administration in the rat. Int. J. Pharm. 132, 123–130.

Hochstrasser, D.F., Harrington, M.G., Hochstrasser, A.C., Miller, M.J., Merril, C.R., 1988. Methods for increasing the resolution of two-dimensional protein electrophoresis. Anal. Biochem. 173, 424–435.

Hussain, N., Florence, A.T., 1996. Invasin-induced oral uptake of nanospheres: utilising bacterial mechanisms of epithelial cell entry. J. Contr. Release 41, S3–S4.

Janes, K.A., Fresneau, M.P., Marazuela, A., Fabra, A., Alonso, M.J., 2001. Chitosan nanoparticles as delivery systems for doxorubicin. J. Contr. Release 73, 255–267.

Jang, M.H., Kweon, M.N., Iwatani, K., Yamamoto, M., Terahara, K., Sasakawa, C., Suzuki, T., Nochi, T., Yokota, Y., Rennert, P.D., Hiroi, T., Tamagawa, H., Iijima, H., Kunisawa, J., Yuki, Y., Kiyono, H., 2004. Intestinal villous M cells: an antigen entry site in the mucosal epithelium. Proc. Natl. Acad. Sci. U.S.A. 101, 6110–6115.

Jani, P., Halbert, G.W., Langridge, J., Florence, A.T., 1989. The uptake and translocation of latex nanospheres and microspheres after oral administration to rats. J. Pharm. Pharmacol. 41, 809–812.

Jepson, M.A., Clark, M.A., Foster, N., Mason, C.M., Bennett, M.K., Simmons, N.L., Hirst, B.H., 1996. Targeting to intestinal M cells. J. Anat. 189 (Pt 3), 507–516.

Jepson, M.A., Simmons, N.L., O'Hagan, D.T., Hirst, B.H., 1993a. Comparison of poly(DL-lactide-co-glycolide) and polystyrene microsphere targeting to intestinal M cells. J. Drug Target 1, 245–249.

Jepson, M.A., Simmons, N.L., Savidge, T.C., James, P.S., Hirst, B.H., 1993b. Selective binding and transcytosis of latex microspheres by rabbit intestinal M cells. Cell Tissue Res. 271, 399–405.

Keegan, M.E., Whittum-Hudson, J.A., Mark Saltzman, W., 2003. Biomimetic design in microparticulate vaccines. Biomaterials 24, 4435–4443.

Kerneis, S., Bogdanova, A., Kraehenbuhl, J.P., Pringault, E., 1997. Conversion by Peyer's patch lymphocytes of human enterocytes into M cells that transport bacteria. Science 277, 949–952.

Kraehenbuhl, J.P., Neutra, M.R., 1992. Transepithelial transport and mucosal defence. II. Secretion of IgA. Trends Cell Biol. 2, 170–174.

Kraehenbuhl, J.P., Neutra, M.R., 2000. Epithelial M cells: differentiation and function. Annu. Rev. Cell Dev. Biol. 16, 301–332.

Larhed, A.W., Artursson, P., Bjork, E., 1998. The influence of intestinal mucus components on the diffusion of drugs. Pharm. Res. 15, 66–71.

Lentner, C., 1981. Geigy Scientific Tables, 6 vols., 8th ed. West Caldwell, NJ, CIBA-Geigy, 1991–1993.

Muller, R.H., Ruhl, D., Luck, M., Paulke, B.R., 1997. Influence of fluorescent labelling of polystyrene particles on phagocytic uptake, surface hydrophobicity, and plasma protein adsorption. Pharm. Res. 14, 18–24.

Neutra, M.R., Mantis, N.J., Frey, A., Giannasca, P.J., 1999. The composition and function of M cell apical membranes: implications for microbial pathogenesis. Semin. Immunol. 11, 171–181.

Ouzilou, L., Caliot, E., Pelletier, I., Prevost, M.C., Pringault, E., Colbere-Garapin, F., 2002. Poliovirus transcytosis through M-like cells. J. Gen. Virol. 83, 2177–2182.

Owen, R.L., 1999. Uptake and transport of intestinal macromolecules and microorganisms by M cells in Peyer's patches—a personal and historical perspective. Semin. Immunol. 11, 157–163.

Rescigno, M., Urbano, M., Valzasina, B., Francolini, M., Rotta, G., Bonasio, R., Granucci, F., Kraehenbuhl, J.P., Ricciardi-Castagnoli, P., 2001. Dendritic cells express tight junction proteins and penetrate gut epithelial monolayers to sample bacteria. Nat. Immunol. 2, 361–367.

Ruponen, M., Honkakoski, P., Tammi, M., Urtti, A., 2004. Cell-surface glycosaminoglycans inhibit cation-mediated gene transfer. J. Gene Med. 6, 405–414.

Thanou, M., Verhoef, J.C., Junginger, H.E., 2001. Oral drug absorption enhancement by chitosan and its derivatives. Adv. Drug Deliv. Rev. 52, 117–126.

Vila, A., Sanchez, A., Tobio, M., Calvo, P., Alonso, M.J., 2002. Design of biodegradable particles for protein delivery. J. Contr. Release 78, 15–24.

Wong, N.A., Herriot, M., Rae, F., 2003. An immunohistochemical study and review of potential markers of human intestinal M cells. Eur. J. Histochem. 47, 143–150.